AIAA 81-0221R

Aircraft Lateral Parameter Estimation from Flight Data with Unsteady Aerodynamic Modeling

William R. Wells*
Wright State University, Dayton, Ohio
Siva S. Banda†
Air Force Wright Aeronautical Laboratories, Wright Patterson Air Force Base, Ohio
and
David L. Quam‡
University of Dayton, Dayton, Ohio

An unsteady aerodynamic model for aircraft lateral motion was considered in the development of a parameter extraction algorithm in the frequency domain. This algorithm was applied to flight test data. The data were transformed into the frequency domain by the use of fast Fourier transform (FFT) algorithms. The results indicate that modeling of unsteady aerodynamics results in significant differences in the parameters C_{l_r}, C_{n_r}, and $C_{l_{\delta_r}}$ in various flights. Also investigated was the sensitivity of the extracted parameters to the control input with the inclusion of unsteady aerodynamic modeling.

Nomenclature

b = span of the surface, ft
$\bar{c}$ = mean geometric chord, ft
F = constant in indicial sidewash equation
g = acceleration due to gravity, ft/s^2
I_x = roll moment of inertia, slug-ft^2
I_z = yaw moment of inertia, slug-ft^2
l_v, z_v = coordinates of the quarter-chord point of the mean chord of the vertical tail with respect to the center of gravity of the airplane, ft
m = mass, slug
M = moment, lb-ft
p = rate of roll, rad/s
$\bar{q}$ = dynamic pressure = $\frac{1}{2}\rho V^2$, lb/ft^2
r = rate of yaw, rad/s
S = area of the surface, ft^2
t = time, s
V = freestream velocity, ft/s
x = state vector
y,z = constants in indicial sideforce equation
β = sideslip angle, rad
δ_a = aileron deflection, rad
δ_r = rudder deflection, rad
$\Delta C_y(t)$ = indicial sideforce function
$\Delta\sigma(t)$ = indicial sidewash function
θ = parameter vector
ρ = air density, slug/ft^3
σ = sidewash angle, rad
τ = dummy variable
ϕ = roll angle, rad
ω = angular frequency, rad/s
C_l = rolling moment coefficient, $M_x/\bar{q}S_w\bar{c}_w$
C_n = yawing moment coefficient, $M_z/\bar{q}S_w\bar{c}_w$
C_y = sideforce coefficient, sideforce/$\bar{q}S_w$
C_{y_β} = $\partial C_y/\partial\beta$
C_{y_p} = $\partial C_y/\partial(pb_w/2V)$
$C_{y_{\delta_r}}$ = $\partial C_y/\partial\delta_r$
C_{l_β} = $\partial C_l/\partial\beta$
C_{l_p} = $\partial C_l/\partial(pb_w/2V)$
C_{l_r} = $\partial C_l/\partial(rb_w/2V)$
$C_{l_{\delta_a}}$ = $\partial C_l/\partial\delta_a$
$C_{l_{\delta_r}}$ = $\partial C_l/\partial\delta_r$
C_{n_β} = $\partial C_n/\partial\beta$
C_{n_p} = $\partial C_n/\partial(pb_w/2V)$
C_{n_r} = $\partial C_n/\partial(rb_w/2V)$
$C_{n_{\delta_a}}$ = $\partial C_n/\partial\delta_a$
$C_{n_{\delta_r}}$ = $\partial C_n/\partial\delta_r$

Subscripts

w, f = wing/body combination
ss = steady state (no unsteady aerodynamic effects)
v = vertical tail

Superscripts

$(\tilde{\ })$ = Fourier transform of the variable in parenthesis
$(\ )^*$ = transpose conjugate of the variable in parenthesis

Presented as Paper 81-0221 at the AIAA 19th Aerospace Sciences Meeting, St. Louis, Mo., Jan. 12-15, 1981; submitted March 3, 1981; revision received July 27, 1981.

*Chairman, Department of Engineering. Associate Fellow AIAA.
†Aerospace Engineer, Flight Dynamics Laboratory. Member AIAA.
‡Associate Professor. Member AIAA.

Introduction

In recent years simplified longitudinal unsteady aerodynamic models have been developed and applied in longitudinal aircraft parameter identification studies.[1-2] Due to the success in the longitudinal case, a preliminary attempt to develop a simplified model for unsteady effects in lateral aircraft dynamics was made in Ref. 3. In that reference the unsteady aerodynamics associated with the sideslipping flight was considered. The approach was to draw an analogy between sidewash in lateral flight to downwash in longitudinal flight in order to obtain a simple mathematical model for unsteadiness. The objective of this paper is to extend the studies of Ref. 3 and to develop a parameter estimation algorithm in the frequency domain based on the maximum likelihood estimation technique and to assess the importance of unsteady aerodynamic modeling on the aircraft lateral parameter estimates.

Force and Moment Modeling

Unsteadiness is introduced into the lateral dynamics via the indicial sidewash and sideforce produced by a unit step change in sideslip angle. Due to changes in the flowfield from the wing, fuselage, and possible propeller slipstream, the effective angle of attack of the vertical tail differs from the sideslip angle by the sidewash angle σ. Assuming an analogy between downwash in longitudinal flight and sidewash in lateral flight, an expression for indicial sidewash function for a unit step change in sideslip angle at the wing can be written as[3]

$$\Delta\sigma_{l_v}(t) = \left(\frac{\partial\sigma}{\partial\beta}\right)_{ss,l_v}\left[1 - \frac{F}{\left(\frac{l_v \cos(1)}{\bar{c}_w} - 1 - \frac{Vt}{2\bar{c}_w}\right)}\right] \tag{1}$$

The above equation is the same as that given in Ref. 3 with the exception of the exponentially decreasing term included there. The exponential term was not included here since its magnitude is negligible compared to the other terms in the expression.

Analogous to the approximate indicial lift function in Ref. 1, an approximate expression for the indicial sideforce function due to a unit step change in the effective angle of attack at the vertical tail was assumed to be in the form

$$(\Delta C_y)_v(t) = (C_{y_\beta})_{ss,v}\left[1 - y\exp\left(-z\frac{Vt}{\bar{c}_{v/2}}\right)\right] \tag{2}$$

The sidewash and the vertical tail contributions to the sideforce for arbitrary changes in sideslip angle were assumed as

$$\sigma_{l_v}(t) = \int_0^t \Delta\sigma_{l_v}(t-\tau)\dot{\beta}(\tau)\mathrm{d}\tau \tag{3}$$

$$(C_y)_v(t) = \int_0^t (\Delta C_y)_v(t-\tau)\left[\dot{\beta}(\tau) - \dot{\sigma}_{l_v}(\tau)\right]\mathrm{d}\tau \tag{4}$$

The contribution of the vertical tail to yawing moment and rolling moment are given in Ref. 3.

Lateral Equations of Motion

The coupled perturbed equations describing the lateral dynamics of the aircraft are

$$\dot{\beta}(t) = \frac{g}{V}\phi(t) - r(t) + \frac{\rho V S_w}{2m}C_y(t) \tag{5}$$

$$\dot{p}(t) = \frac{\rho V^2 S_w b_w}{2I_x}C_l(t) \tag{6}$$

$$\dot{r}(t) = \frac{\rho V^2 S_w b_w}{2I_z}C_n(t) \tag{7}$$

$$\dot{\phi}(t) = p(t) \tag{8}$$

The force and moment coefficients expressed in Eqs. (5-8) contain the contributions due to the vertical tail discussed previously and additional effects due to control surface deflections, wing/body combinations, etc.[3]

Maximum Likelihood Estimation Algorithm

Due to the computational difficulties associated with the time domain description of the equations of motion, the estimation algorithm was developed in the frequency domain. The Fourier transform pair associated with a function $x(t)$ is

$$\tilde{x}(j\omega) = \int_0^\infty x(t)e^{-j\omega t}\mathrm{d}t$$

$$x(t) = \frac{1}{2\pi}\int_{-\infty}^{\infty} x(j\omega)e^{j\omega t}\mathrm{d}\omega \tag{9}$$

The transformed equivalent of Eqs. (5-8) can be written in the following state space notation for estimation purposes

$$\tilde{x}(j\omega) = D(j\omega,\theta)G(\theta)\tilde{u}(j\omega) \tag{10}$$

where

$$\tilde{x}(j\omega) = [\tilde{\beta}(j\omega), \tilde{p}(j\omega), \tilde{r}(j\omega), \tilde{\phi}(j\omega)]^T \tag{11}$$

$$\tilde{u}(j\omega) = [\tilde{\delta}_r(j\omega), \tilde{\delta}_a(j\omega)]^T \tag{12}$$

θ is the vector whose components are the parameters to be estimated. $D(j\omega,\theta)$ is an appropriately chosen matrix containing stability derivatives and $G(\theta)$ is a matrix of control derivatives. Flight data are in the form of time histories of β, p, r, ϕ, δ_r, and δ_a. These are converted into the frequency domain. It is assumed that the measured data are known at equally spaced instants $i\Delta t$, $i=0,1,\ldots,(N-1)$ where N is number of data points.

The state space form of the frequency spectrum for the measured output is

$$\tilde{z}(n) = H\tilde{x}(n) + \tilde{v}(n) \tag{13}$$

where $\tilde{v}$ is a vector of measurement noise assumed to be Gaussian white with zero mean and variance R. H is an appropriately chosen matrix of known parameters.

Klein[4] has shown that the maximum likelihood estimate of θ is given according to

$$\hat{\theta} = \theta_0 + \Delta\hat{\theta} \tag{14}$$

where

$$\Delta\hat{\theta} = \left[\mathrm{Re}\sum_{n=1}^{N}\left(\frac{\partial\tilde{v}}{\partial\theta}\right)^*\hat{R}^{-1}\left(\frac{\partial\tilde{v}}{\partial\theta}\right)\right]^{-1}\left[\mathrm{Re}\sum_{n=1}^{N}\left(\frac{\partial\tilde{v}}{\partial\theta}\right)^*\hat{R}^{-1}\tilde{v}\right] \tag{15}$$

$$\tilde{v}(n) = \tilde{z}(n) - \tilde{x}(n,\theta_0) \tag{16}$$

$$R = \mathrm{diag}\left[\frac{1}{N}\sum_{n=1}^{N}\tilde{v}(n)\tilde{v}^*(n)\right] \tag{17}$$

In Eq. (15), the symbol Re ( ) denotes the real part of the complex number in the parenthesis.

Results and Discussion

A low-wing, single-engine, general aviation airplane is used in the flight test. The characteristics of the aircraft and flight conditions are shown in Tables 1 and 2. The lateral mode was excited separately primarily from trimmed level flight. Both the rudder and aileron inputs were applied simultaneously. In each run β, p, r, ϕ, δ_r, and δ_a were measured. The measured

Table 1 Characteristics of the aircraft used in test flights

Item	Wing	Vertical tail
S, ft^2	146.0	13.1
c, ft	4.4	4.6
b, ft	32.7	4.6

$l_v = 15.08$ ft

$z_v = 2.9$ ft

$(C_{l_\beta})_{w,f} = -0.0906$[a]

$y = 0.067$[b]

$\left(\frac{\partial\sigma}{\partial\beta}\right)_{ss,l_v} = 0.0647$[a]

$z = 0.62$[b]

$(C_{n_\beta})_{w,f} = -0.0218$[a]

[a]From Ref. 7. [b]From Ref. 1.

Table 2 Flight conditions, average mass, and inertia characteristics of airplane in test flights

Characteristic	Flight: runs 21:26,27	26:23,24
I_x, slug-ft^2	1487.8	1498.8
I_z, slug-ft^2	2797.8	2805.2
m, slug	71.16	71.9
ρ, slug/ft^3	0.00215	0.002101
V, ft/s	152	156

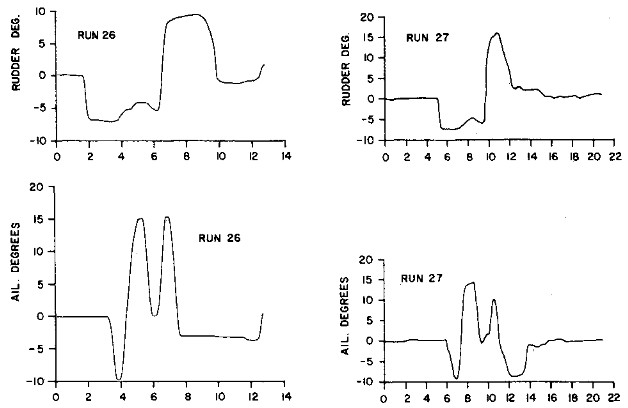

Fig. 1 Control inputs used in the flight tests, flight 21.

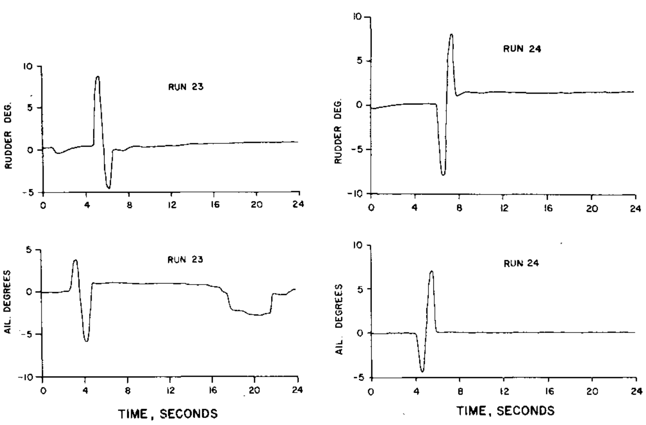

Fig. 2 Control inputs used in the flight tests, flight 26.

Table 3 Parameters extracted from flight 21, run 26

Parameter	Estimated value[a] (1)	(2)	Change, %
$(C_{y_\beta})_{ss,v}$	−0.3671 (±0.0061)[b]	−0.3636 (±0.0051)[b]	0.97
C_{l_r}	0.1706 (±0.0253)	0.1891 (±0.0248)	9.8
$C_{l_{\delta_a}}$	−0.2279 (±0.0029)	−0.2268 (±0.0029)	0.49
$C_{l_{\delta_r}}$	0.0383 (±0.0042)	0.0389 (±0.0043)	1.5
C_{n_r}	−0.2404 (±0.0118)	−0.2283 (±0.0091)	5.3
$C_{n_{\delta_a}}$	0.0322 (±0.0015)	0.0298 (±0.0014)	8
$C_{n_{\delta_r}}$	−0.0729 (±0.0030)	−0.0695 (±0.0028)	4.8
F	0.3280 (±0.5479)	–	–

[a](1) = with unsteady terms retained. (2) = with unsteady terms omitted. [b]Standard deviation.

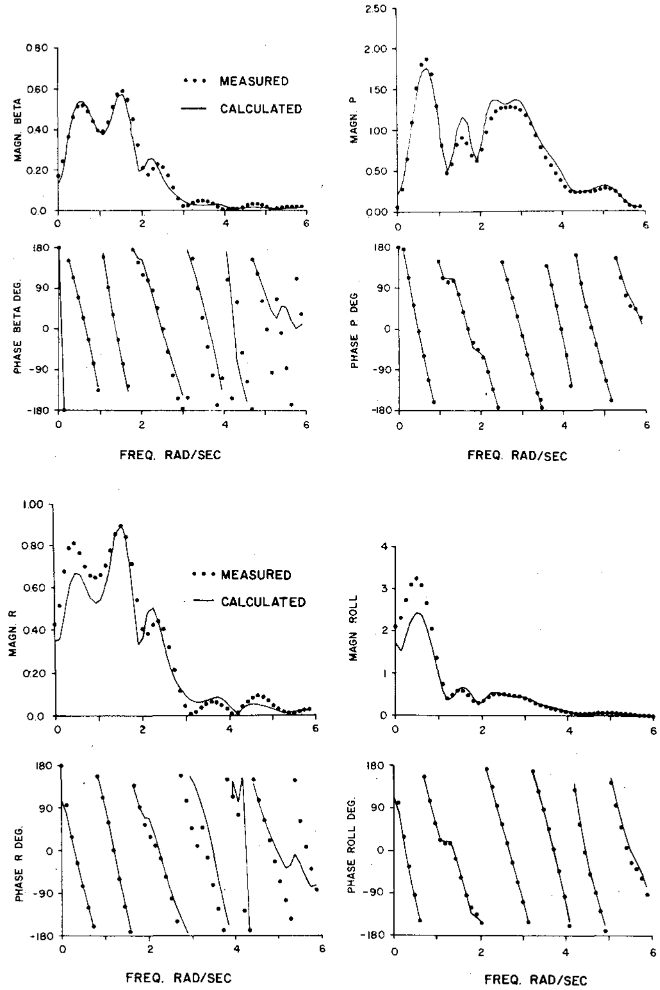

Fig. 3 Comparison of transformed response for the estimates of Table 3, unsteady terms retained.

data were sampled at the rate of 20 samples/s. The data were preprocessed to remove constant bias errors. In each flight two runs were made with two different sets of control inputs. Figures 1 and 2 show the control inputs used in flights 21 and 26.

Since the parameter extraction is done in the frequency domain, the measured data were converted into the frequency domain by using fast Fourier transform (FFT) algorithms.[5] The transformed data of $\tilde{\beta}$, $\tilde{p}$, $\tilde{r}$, and $\tilde{\phi}$ for flight 21, run 26 is shown in Fig. 3. The data points were obtained at every 0.12 rad/s.

In the parameter extraction process, two cases were considered. The first case was the estimation of parameters using the extraction algorithm with unsteady aerodynamic terms retained. The second case was the estimation using the algorithm with unsteady terms omitted. An initial guess for the parameters to be estimated was given to start the identification process.

The agreement between the measured data and the responses obtained from the final estimated values of the parameters for the first case is shown in Fig. 3. The results of parameter extraction for flight 21, runs 26, 27 and flight 26, runs 23, 24 are shown in Tables 3-6, respectively.

While handling the real flight data, several difficulties were encountered. One was that the frequency response curves were not as smooth as those one would obtain when working with simulated data. All of the input forms resulted in strong correlations between C_{l_p}, $C_{l_{\delta_a}}$ and C_{n_p}, $C_{n_{\delta_a}}$. Consequently, the values of C_{l_p} and C_{n_p} were fixed at those given by other methods.[6]

The inclusion of unsteady aerodynamics did effect the values of the parameters, particularly in C_{l_r} (Table 3), C_{n_r}

Table 4 Parameters extracted from flight 21, run 27

Parameter	Estimated value[a] (1)	(2)	Change, %
$(C_{y_\beta})_{ss,v}$	−0.3849	−0.3850	0.03
	(±0.0091)[b]	(±0.0082)[b]	
C_{l_r}	0.2601	0.2555	1.8
	(±0.0393)	(±0.0384)	
$C_{l_{\delta_a}}$	−0.2478	−0.2472	0.25
	(±0.0055)	(±0.0054)	
$C_{l_{\delta_r}}$	−0.0479	0.0476	0.63
	(±0.0059)	(±0.0058)	
C_{n_r}	−0.2307	−0.2235	3.2
	(±0.0172)	(±0.0149)	
$C_{n_{\delta_a}}$	−0.0348	0.0347	0.29
	(±0.0016)	(±0.0015)	
$C_{n_{\delta_r}}$	−0.0727	−0.0725	0.28
	(±0.0047)	(±0.0046)	
F	0.0757	−	−
	(±0.6064)		

[a](1) = with unsteady terms retained. (2) = with unsteady terms omitted. [b]Standard deviation.

Table 5 Parameters extracted from flight 26, run 23

Parameter	Estimated value[a] (1)	(2)	Change, %
$(C_{y_\beta})_{ss,v}$	−0.4004	−0.3884	3
	(±0.0136)[b]	(±0.0088)[b]	
C_{l_r}	0.1651	0.1571	5
	(±0.0316)	(±0.0323)	
$C_{l_{\delta_a}}$	−0.2507	−0.2521	0.5
	(±0.0060)	(±0.0067)	
$C_{l_{\delta_r}}$	0.0120	0.0132	9
	(±0.0079)	(±0.0088)	
C_{n_r}	−0.2224	−0.2029	9.6
	(±0.0190)	(±0.0144)	
$C_{n_{\delta_a}}$	0.0372	0.0371	0.2
	(±0.0043)	(±0.0043)	
$C_{n_{\delta_r}}$	−0.0680	−0.0683	0.4
	(±0.0062)	(±0.0061)	
F	0.6664	−	−
	(±0.9999)		

[a](1) = with unsteady terms retained. (2) = with unsteady terms omitted. [b]Standard deviation.

Table 6 Parameters extracted from flight 26, run 24

Parameter	Estimated value[a] (1)	(2)	Change, %
$(C_{y_\beta})_{ss,v}$	−0.3957	−0.3804	4
	(±0.0114)[b]	(±0.0086)[b]	
C_{l_r}	0.1333	0.1230	8.4
	(±0.0297)	(±0.0283)	
$C_{l_{\delta_a}}$	−0.2211	−0.2199	0.5
	(±0.0108)	(±0.0140)	
$C_{l_{\delta_r}}$	0.0137	0.0176	22.2
	(±0.0067)	(±0.0077)	
C_{n_r}	−0.2110	−0.1768	19.3
	(±0.0212)	(±0.0143)	
$C_{n_{\delta_a}}$	0.0415	0.0419	0.9
	(±0.0067)	(±0.0072)	
$C_{n_{\delta_r}}$	−0.0589	−0.0579	1.7
	(±0.0057)	(±0.0057)	
F	0.9193	−	−
	(±1.345)		

[a](1) = with unsteady terms retained. (2) = with unsteady terms omitted. [b]Standard deviation.

Table 7 Variation in the extracted parameters for flight 21, runs 26 and 27

Parameter	Unsteady terms retained[a]	Unsteady terms omitted[a]
$(C_{y_\beta})_{ss,v}$	0.0178	0.0214
	(4.6)[b]	(5.5)[c]
C_{l_r}	0.0895	0.0664
	(34.4)	(2.6)
$C_{l_{\delta_a}}$	0.0199	0.0204
	(8)	(8.2)
$C_{l_{\delta_r}}$	0.0096	0.0087
	(20)	(18.3)
C_{n_r}	0.0097	0.0048
	(4.2)	(2.1)
$C_{n_{\delta_a}}$	0.0026	0.0049
	(7.5)	(14.1)
$C_{n_{\delta_r}}$	0.0002	0.0030
	(0.3)	(4.1)

[a]Change from Table 3 to Table 4. [b]% variation, % of column 2 of Table 4. [c]% variation, % of column 3 of Table 4.

Table 8 Variation in the extracted parameters for flight 26, runs 23 and 24

Parameter	Unsteady terms retained[a]	Unsteady terms omitted[a]
$(C_{y_\beta})_{ss,v}$	0.0047	0.008
	(1.2)[b]	(2.1)[c]
C_{l_r}	0.0318	0.0341
	(23.9)	(27.7)
$C_{l_{\delta_a}}$	0.0296	0.0322
	(13.4)	(14.6)
$C_{l_{\delta_r}}$	0.0017	0.0044
	(12.4)	(25)
C_{n_r}	0.0114	0.0261
	(5.4)	(14.1)
$C_{n_{\delta_a}}$	0.0043	0.0048
	(10.4)	(11.5)
$C_{n_{\delta_r}}$	0.0091	0.0104
	(15.4)	(18)

[a]Change from Table 5 to Table 6. [b]% variation, % of column 2 of Table 6. [c]% variation, % of column 3 of Table 6.

(Tables 4 and 5), and $C_{l_{\delta_r}}$ (Table 6). The confidence on the estimate of F is seen to be poor from Tables 3-6. This means that the parameter F is highly sensitive to the unsteadiness in the model. One way to overcome this is by estimating F by other means such as wind-tunnel results. The variation in the extracted parameters for the two different control inputs for flight 21 is shown in Table 7 and for flight 26 in Table 8. From Table 7 the extracted parameters show less variation in $(C_{y_\beta})_{ss,v}$, $C_{l_{\delta_a}}$, $C_{n_{\delta_a}}$, and $C_{n_{\delta_r}}$ for different control inputs when the unsteady aerodynamic terms were retained in the estimation algorithm. It is interesting to note from Table 8 that all of the extracted parameters show less variation when the unsteady effects are taken into account.

Conclusion

A model to account for unsteadiness in the sideslipping flight of an aircraft is utilized in a maximum likelihood estimation algorithm to estimate the aircraft stability and control derivatives. This algorithm was applied in the frequency domain to flight data. Use of the unsteady aerodynamic model in the algorithm resulted in significant differences in some of the parameters such as C_{l_r}, C_{n_r}, and $C_{l_{\delta_r}}$ in various flights. For the cases considered, the extracted parameters showed less variation to the shape of the control inputs when the unsteady effects were accounted for in the estimation algorithm.

References

[1]Queijo, M.J., Wells, W.R., and Keskar, D.A., "Approximate Indicial Lift Function for Tapered, Swept Wings in Incompressible Flow," NASA TP 1241, Aug. 1978.

[2]Queijo, M.J., Wells, W.R., and Keskar, D.A., "Inclusion of Unsteady Aerodynamics in Longitudinal Parameter Estimation From Flight Data," NASA TP 1536, Dec. 1979.

[3]Wells, W.R., Banda, S.S., and Quam, D.L., "Model for Unsteady Effects in Lateral Dynamics for Use in Parameter Estimation," *Journal of Aircraft*, Vol. 17, Sept. 1980, pp. 702-704.

[4]Klein, V., "Aircraft Parameter Estimation in Frequency Domain," *Proceedings of AIAA Atmospheric Flight Mechanics Conference*, Aug. 1978, pp. 140-147 (available as AIAA Paper 78-1344).

[5]Oran Brigham, E., *The Fast Fourier Transform*, Prentice-Hall, Inc., Englewood Cliffs, N.J., 1974.

[6]Klein, V., "Determination of Stability and Control Parameters of a Light Airplane from Flight Data Using Two Estimation Methods," NASA TP 1306, March 1979.

[7]Hoak, D.E. et al., "USAF Stability and Control DATCOM," Flight Control Division, Air Force Flight Dynamics Laboratory, Wright-Patterson Air Force Base, Ohio, April 1976.